Abstract

The interactions of K^- mesons at 1.5 GeV/c beam momentum with protons were observed using photographs taken of the 25" hydrogen bubble chamber operating at the Lawrence Berkeley Laboratory Bevatron. The branching ratio of the K^- tau mode decay was found to be $5.98 \pm .55$ %, and the calculated total cross section for 1.5 GeV/c K^- interactions with protons was 56.6 ± 3.5 mb. The K^- meson lifetime was calculated to be $(1.256 \pm .061) * 10^{-8}$ seconds. All are in good agreement with known values. Also, 20 GeV photon-proton interactions were observed using photographs from the 40" bubble chamber at the Stanford Linear Accelerator Center (SLAC). The total production cross section of strange particles in 20 GeV photon-proton interactions was found to be 12.91 ± 1.9 μb. This is in the range of acceptable values.

Introduction

The principal decay modes of the K^- meson are[1]:

$$K^- \rightarrow \mu^- \nu_\mu \qquad BR = 63.5\%$$
$$K^- \rightarrow \pi^- \pi^0 \qquad BR = 21.2\%$$
$$K^- \rightarrow \pi^- \pi^- \pi^+ \qquad BR = 5.6\%$$
$$K^- \rightarrow e^- \pi^0 \nu \qquad BR = 4.9\%$$
$$K^- \rightarrow \mu^- \pi^0 \nu \qquad BR = 3.2\%$$
$$K^- \rightarrow \pi^- \pi^0 \pi^0 \qquad BR = 1.7\%$$

listed in order of greatest likelihood of occurrence. The branching ratio, designated as BR for each mode, tells the fraction of all possible decays that each mode represents. The branching ratio for the decay $K^- \rightarrow \pi^- \pi^- \pi^+$ is calculated in this experiment. When a beam of particles, in this case K^- mesons, are incident on a target, such as hydrogen nuclei, there is a probability that the particle will interact with the target. A parameter which characterizes all such interactions is the 'total cross section', which has units of area. It is customary to quote subatomic cross sections in 'barns', where 1 b = 10^-24 cm^2 = 100 fm^2 . However, the total cross section is an effective scattering area, not an actual area. It is a function of the type and energy of the particles reacting, and is only occasionally equal to the actual geometrical area of the scattering center. Unstable particles such as the K^- meson decay after some mean lifetime. This lifetime is easy to calculate using special relativity, once the physicist understands how his beams of particles are being attenuated as a function of distance traveled. Such a relation will be derived in the following section.

Photons of very high energy are observed to exhibit "hadronlike" properties. Namely, they exhibit hadronic internal structure, and can interact via the strong (hadronic) interactions. Due to the uncertainty principle, $\Delta E \Delta t \leq \hbar$, a high energy photon can have an energy fluctuation (and hence mass) for a very short time. The photon transforms into a "virtual" hadron briefly, which can subsequently interact with other hadrons, such as protons. However, due to the very small times permissible by the uncertainty principle, this hadronic nature of the photon only manifests itself at high energies, in this case 20 GeV. The hadronic reactions of photons with protons sometimes produce strange particles, which are so named because they are produced by the strong interaction, but only decay via weak interactions. The total cross section for strange particle photoproduction at 20 GeV is calculated in this experiment.

These observations and calculations are carried out using bubble chamber photographs, where incident particles such as K^- mesons or photons collide with protons of the liquid hydrogen inside the bubble chamber. Charged particles passing through the liquid hydrogen cause ionization, nucleation, and hence leave tracks of bubbles which reveal the interactions.

Theory

The cross section and mean life of the K^- meson can be calculated using the attenuation formula for the decrease in observed K^- as a function of x across the observed bubble chamber region (called the fiducial region). The formula can be derived as follows :

ATTENUATION RATE DUE TO INTERACTIONS IS $\equiv \frac{dN_I}{dx}$,

$$\frac{dN_I}{dx} \propto \left(\begin{matrix}\text{\# of Scattering centers}\\ \text{(nuclei) in target area}\end{matrix}\right) \cdot \left(\begin{matrix}\text{\# of } K^-\\ \text{present}\end{matrix}\right) \cdot \left(\begin{matrix}\text{effective area of each}\\ \text{scattering center}\end{matrix}\right)$$

$$= \left(\frac{\text{Avagadro's Number} \cdot \text{density of liquid Hydrogen}}{\text{Atomic Number of Hydrogen}}\right)(-N)\left(\begin{matrix}\text{Total Scattering}\\ \text{cross-section}\end{matrix}\right)$$

$$= \left(\frac{N_A \rho}{A}\right)(-N)(\sigma)$$

$$\frac{dN_I}{dx} = -N\left(\frac{N_A \rho \sigma}{A}\right)$$

beam attenuation due to decays $\equiv \frac{dN_D}{dx}$

$$\frac{dN_D}{dx} \propto \left(\begin{matrix}\text{Number of } K^-\\ \text{present}\end{matrix}\right)\left(\frac{1}{\text{proper time spent in fiducial volume}}\right)$$

$$= -N\left(\frac{1}{\beta\gamma c\tau}\right)$$

, $\tau \equiv$ lifetime of particle (mean)

$\beta\gamma = \frac{P}{Cm}$ relativistic correction for time dilation

$$\frac{dN_D}{dx} = \frac{-N}{\beta\gamma c\tau}$$

$$\text{Total attenuation} = \frac{dN}{dx} = \frac{dN_I}{dx} + \frac{dN_D}{dx}$$

$$= -N\left[\frac{1}{\beta\gamma c\tau} + \frac{N_A \rho\sigma}{A}\right]$$

$$\int^{N} \frac{dN}{N} = -\int^{x} \left[\frac{1}{\beta\gamma c\tau} + \frac{N_A \rho\sigma}{A}\right] dx$$

It was shown in the previous calculation that a photon cannot produce a real pair of massive particles in free space. A nucleus must be present to take up the momentum in order to satisfy energy-momentum conservation. However, the uncertainty principle : $\Delta E \Delta t \leq \hbar$ allows for a quantum fluctuation in energy, which can exist for a time less than $\hbar/\Delta E$. It has been observed in this part of the experiment that a photon can interact via hadronic (strong) processes; and shows hadronic structure at high energies. So by the uncertainty principle, a photon can produce a "virtual" particle with the same quantum numbers as the photon, with energy ΔE for a short time. This virtual hadron could interact hadronically, and probe other nuclei to distances limited in the time of travel given by $\hbar/\Delta E$. The energy of the virtual hadron is $\Delta E = E_h - E_\gamma$. Relativistically, $P_h = P_\gamma = \frac{E_\gamma}{c}$, and this is $\Delta E = (E_\gamma^2 + m_h^2 c^4) - E_\gamma$. Thus, the hadron can exist for a time of :

$$\Delta t \leq \frac{\hbar}{\sqrt{E_\gamma^2 + m_h^2 c^4} - E_\gamma}$$

The hadron could travel at most the speed of light, so the maximum distance the hadron could "probe" would be:

$$d_{max} = c(\Delta t) = \frac{\hbar c}{\sqrt{E_\gamma^2 + m_h^2 c^4} - E_\gamma}$$

The smallest mass hadron with the same spin as the photon is the rho meson, with m_h = 776 Mev/c^2. Using the rho meson for this model, the probing distance at a photon energy of 2 eV is :

$$d = \frac{6.582 \times 10^{-22} \text{ MeV-sec } (3 \times 10^{8} \text{ m/s})}{\sqrt{(2 \times 10^{-6} \text{ MeV})^2 + 776 \text{ MeV}} - (2 \times 10^{-6} \text{ MeV})} = 2.54 \times 10^{-16} \text{ m}$$

$$= .25 \text{ fm}$$

and at a photon energy of 20 MeV is:

$$d = \frac{6.582\times10^{-22}(3\times10^{8})}{\sqrt{(20.0)^2+(776)^2}-(20.0)} = 2.61\times10^{-16}\,m = .26\ fm.$$

These are not significant, considering the proton radius is of order 0.7 fm. However, at a high photon energy of 20 GeV, as is the case in this experiment, the probing distance is:

$$d = \frac{6.582\times10^{-22}\ MeV\text{-}sec\ (3\times10^{8}\ m/sec)}{\sqrt{(20\times10^{3}\ MeV)^2-(776\ MeV)^2}-(20\times10^{3}\ MeV)} = 1.31\times10^{-14}\,m = 13.1\ f$$

This is far enough to probe deep within the largest nuclei. Therefore it becomes clear that we need different models to describe the photon interaction with matter at different energy regime.

Consider (prob. 4.4) treating a Feynman diagram as a wave-function describing an interaction and the wave-function in this case is proportional to the product of the coupling constant at each vertex in the Feynman diagram. Then it becomes possible to compare the total cross section of a gamma-proton collision with that of a pion-proton collision at 20 GeV. The Feynman diagrams for the electromagnetic interaction and hadronic interaction[2] are:

with the coupling constants e, and $f_\pi pp$ at each respective vertex. The square of e, given in dimensionless form, is the fine structure constant $\alpha = e^2/\hbar c = 1/137$ which is of order(0.01). The coupling constant $f_{\pi pp}$ is of order 1, meaning that the strong force is about 100 times greater on average than the electromagnetic force. So, the ratio of the gamma-proton total cross section to the pion-proton total cross section is given by the ratio of the squares of the coupling constants:

$$\frac{\alpha}{f_{\pi pp}} = \frac{(e^2/\hbar c)}{f_{\pi pp}} = \frac{.01}{1} = .01 = \frac{\sigma_{tot\ \gamma p}}{\sigma_{tot\ \pi p}}$$

This makes sense, and can be thought about using a crude geometrical analogy. The pion is a massive particle and it will see an "effective radius" of the proton of approximately 3 fm^2. However, the photon is massless has a much less well defined radius, so it would seem much more "transparent" to the proton. Hence, the gamma-proton cross section would be much lower than the pion-proton cross section.

The production cross section of strange particles in 20 GeV photon-proton reaction can be estimated by considering the two types of strange particles which were observed in this experiment by hadronic photoproduction, the K^+, and the Λ^0. The cross sections are calculated using:[5]

$$\sigma_i(\gamma p \rightarrow S_{tr_i} X) = \frac{N_{strange}}{N_{\substack{total\\ photoproduction\\ observed}}} \cdot \frac{\epsilon}{BR} \cdot \sigma_T$$

where $\epsilon = \dfrac{\text{efficiency of detecting photoproduction events}}{\text{efficiency of detecting strange particle events}} \cong \dfrac{.95}{.75} = 1.25$

AND BR IS THE BRANCHING RATIO OF THE DECAY USED TO IDENTIFY THE STRANGE PARTICLE, AND

σ_T = total photoproduction cross section at 20 GeV

$= 115 \pm 2\ \mu b$ (WOLBERS, 1980) (ref. 5)

USING THE DATA (AND ILLUSTRATIONS IN APPENDIX),

$$\sigma_{K^+} = \frac{2 \text{ events}}{58 \text{ events}} \cdot \frac{1.27}{.635}(115 \pm 2)\ \mu b = (7.93 \pm .14)\ \mu b$$

$$\sigma_{\Lambda^0} = \frac{2 \text{ events}}{58 \text{ events}} \cdot \frac{1.27}{.650}(115 \pm 2)\ \mu b = (4.98 \pm .09)\ \mu b$$

$$\sigma_{tot,\,strange} = \sum_i \sigma_i = \sigma_{K^+} + \sigma_{\Lambda^0} = 12.91 \pm .23\ \mu b$$

NOW RANDOM ERROR IS A FACTOR, SO TAKE

$$\frac{\Delta\sigma}{\sigma} = \frac{\sqrt{n}}{n} = \frac{\sqrt{58}}{58} = .131,$$

$$\Delta\sigma_{K^+} = .14 + 7.93(.131) = 1.18\ \mu b$$

$$\Delta\sigma_{\Lambda^0} = .09 + 4.98(.131) = .742\ \mu b$$

$$\Delta\sigma_{tot} = 1.9\ \mu b$$

$$\Rightarrow \boxed{\sigma_{tot,S} = (12.91 \pm 1.9)\ \mu b}$$

total cross section for strange particle production at 20 GeV.

AN 'ESTIMATE', SINCE

This value of 12.91 microbarns seems reasonable, when considering two well known values[5] for strange particle production at 20 GeV (Wolbers, 1980) :

$$\sigma(\gamma p \to K^0 X) = 9.66 \pm .27 \quad \mu b$$

$$\sigma(\gamma p \to \Lambda X) = 5.60 \pm .18 \quad \mu b \qquad (\text{at } 20\ \text{GeV})$$

Hence, the order of magnitude is correct, and it seems plausible that the total cross section for strange particle production would be in this range.

Results

K^- meson tau mode decay branching ratio : $\boxed{BR = 5.98 \pm .55 \%}$

$BR_{acc} = 5.60$, % DIFF = 6.8 %

Total cross section for 1.5 GeV/c momentum K^- reactions with protons :

$\boxed{\sigma = 56.6 \pm 3.5 \text{ mb}}$ $\sigma_{acc} = 58.0$, % DIFF = 2.4%

K^- mean lifetime : $\boxed{\tau = (1.256 \pm .061) * 10\hat{}-8 \text{ seconds}}$

$\tau_{acc} = 1.240 \times 10^{-8}$ sec , % DIFF = 1.3 %

Production cross section of strange particles in 20 GeV photon-proton interaction:

$\boxed{\sigma_s = 12.91 \pm 1.9 \ \mu b}$ $\sum \sigma_{i,acc} \cong 16 \ \mu b$

Conclusions

The calculated values above agree very well with the accepted values, with percent differences of within 7 %. The strange particle production cross section is in excellent order of magnitude agreement with individual strange particle cross sections. The uncertainty range on the K^- lifetime is illustrative of a large random counting uncertainty, which is expected since only one film scanner performed the entire analysis. Increasing the number of film scanners reduces the random counting error.

gives: $$\ln\left(\frac{N}{N_0}\right) = -\left[\frac{x}{\beta\gamma c\tau} + \frac{N_A \rho \sigma}{A} x\right]$$

$$\frac{N}{N_0} = e^{-\left[\frac{x}{\beta\gamma c\tau} + \frac{N_A \rho \sigma}{A} x\right]}$$

$$\boxed{N = N_0\, e^{-\left(\frac{x}{\beta\gamma c\tau}\right)}\, e^{-\left(\frac{N_A \rho \sigma x}{A}\right)}}$$

define ΔN_I = total number of interactions
ΔN_D = total number of decays, then

$N_0 - N = \Delta N_D$

$N_0 - N = \Delta N_I \rightarrow 2(N_0 - N) = \Delta N_D + \Delta N_I \rightarrow N = N_0 - \left(\frac{\Delta N_I + \Delta N_D}{2}\right)$

The branching ratio of the tau mode decay is just the fraction of the total decays:

$$BR = \frac{Rate(K^- \rightarrow \pi^- \pi^- \pi^+)}{Rate(K^- \rightarrow \text{all decays})}$$

The strange particle production cross section is also a form of a fractional relation, to the total photoproduction cross section, as follows : $\sigma_i = \left(\frac{N_{\text{strange, observed}}}{N_{\text{total photoproduction events}}}\right) \cdot \frac{\epsilon}{BR}\, \sigma_T$

where ϵ is the scanning efficiency correction factor (see calculations),
BR is the strange particle decay mode branching ratio,
σ_T = total strange particle production cross section at given energy.

and $\sigma_{total} = \sum_i \sigma_i$ (over all 'i' strange particles)

The total strange particle production cross section is the sum of the individual strange particle cross sections :

$$\sigma_{tot\ strange} = \sum_i \sigma_i = \sigma_{K\pm} + \sigma_{K^0} + \sigma_\Lambda + \ldots \text{ etc.}$$

Apparatus and Procedure

The photographs of the bubble chambers with particle interactions were scanned using a special film projector. The photographs are easily maneuvered back and forth, and the images can be magnified. 500 frames of K^- meson interactions and 500 frames (photographs) of photon interactions were observed. Decays are distinguished from interactions by using conservation of charge. Since the net initial charge is zero for a K^-p interaction, and +1 for a gamma-proton interaction, the products must have a sum charge of zero or one respectively. Thus if, for example, the K^- meson track is observed to break up into an odd number of paths, this must always be a decay, because the initial charge is -1. All decays are odd, etc.

A sketch of a bubble chamber + description of the process are in order here.

Calculations and Analysis

The branching ratio is found using :

$$BR \equiv \frac{Rate\,(K^- \rightarrow \pi^+\pi^-\pi^-)}{Rate\,(K^- \rightarrow \text{all decays})}$$

$$= \frac{\sum(\text{observed } K^- \rightarrow \pi^-\pi^-\pi^+ \text{ decays})}{\sum(\text{observed decays})}$$

$$= \frac{7}{117}$$

$$\approx .0598$$

$$= \underline{\underline{5.98\ \%}}$$

Random error associated with this figure dominates, because random counting is such a significant portion of this data acquisition process. The probability distribution in this case is the Poisson distribution, given by $P(n) = \frac{(\bar{n})^n}{n!} e^{-(\bar{n})}$ where $\bar{n}$ is the average number of events. The standard deviation is $\sqrt{n}$, and n is just the number of counts, 117. Using $\Delta n = \sqrt{n}$, $\frac{\Delta BR}{BR} = \frac{\Delta n}{n} \longrightarrow \Delta BR = BR\left(\sqrt{n}/n\right)$, gives : $\Delta BR = BR\left(\frac{\sqrt{n}}{n}\right) = (5.98\,\%)\left(\frac{\sqrt{117}}{117}\right) = .55\,\%$.

The final value is then : $\boxed{BR = 5.98 \pm .55\ \%}$. The accepted value[1] is $BR_{acc.} = 5.60\ \%$, which lies within the error range. The percent difference is $\frac{(5.98 - 5.60)(100\%)}{(5.60)} = 6.8\ \%$.

The total cross section for 1.5 Gev/c momentum K^- on protons, and the K^- lifetime are calculated using the beam attenuation formula, derived in the theory section :

$$N = N_0 e^{-\left(\frac{x}{\beta\gamma c\tau}\right)} e^{-\left(\frac{x N_A \sigma \rho}{A}\right)}$$

As was shown, the attenuation rate has contributions due to interactions and decays :

$$\frac{dN_I}{dx} = -N\left(\frac{N_A \sigma \rho}{A}\right) \Longrightarrow \ln\left(\frac{N}{N_0}\right) = \frac{-N_A \sigma \rho (\Delta x)}{A}$$

where N_0 is the initial number of K^- , N is the effective K^- remaining after traveling a distance x through the fiducial volume, and N_A is Avagadro's number. The magnitude of the total cross section is then : $\sigma = \frac{-\ln(N/N_0) A}{N_A \rho (\Delta x)_{FIDUCIAL}}$

where A is 1 g/mole for hydrogen, rho is .06 g/cm^3 for liquid hydrogen, and N_A = 6.022 *10^23 particles/mole. Now, N_0 , the total number of good K^- tracks, was recorded every tenth frame, so the average is :

$$N_0 = \frac{\Sigma(\text{GOOD BEAMS RECORDED})}{50} = 8.90 \text{ tracks}$$

within the fiducial region. N_0(total) = 8.90(500) = 4450 .

Using $N_0 - N_{eff} = \Delta N_I$ = total number of observed interactions:

$$(N_0 - N) = \Delta N_I$$

$$N = N_0 - \Delta N_I$$

$$\frac{N}{N_0} = 1 - \frac{\Delta N_I}{N_0}$$

$$= \left[1 - \frac{268}{4450}\right]$$

However, since $\Delta m_k/m_k$ is much less than $(\Delta n)/n$, use:

$$\Delta\tau = \tau\left(\frac{\Delta m_{k^-}}{m_{k^-}} + \frac{1}{2}\frac{\Delta n}{n} \right) = 1.256\times10^{-8}\left(\frac{2\,\text{meV}}{494\,\text{meV}} + \frac{1}{2}\frac{\sqrt{117}}{117} \right) = .061\times10^{-8}\,\text{s}$$

$\Delta(\Delta x)$ of the fiducial region is not important here, because the fiducial region is very clearly marked, and only seldom do events (if ever) occur so close to the boundary as to be considered uncertain. The final value of K^- lifetime is:

$$\boxed{\tau = (1.256 \pm .061) * 10^{-8} \text{ seconds}}$$

The accepted value[3] of τ is 1.240 * 10^-8 seconds. This is within the error range above, and the percent difference is $\frac{(1.256 - 1.240)}{(1.240)}(100\%) = 1.3\%$.

Further consideration of systematic scanning error (optional problem #2) due to small angle $K^- \to \mu^- \nu_\mu$ decays (the most common decay mode) is carried out by calculating the maximum muon momentum due to a $K^- \to \mu^- \nu_\mu$ decay. This is best done using energy-momentum four vectors, which transform according to the lorentz transformations. The invariant inner product of the 4-vector can be exploited by evaluating it in any reference frame which is most convenient (usually the center of mass (CM) frame). The decay is:

$K^- \to \mu^- \nu_\mu$:

ν_μ NEUTRINO : $m_\nu = 0$

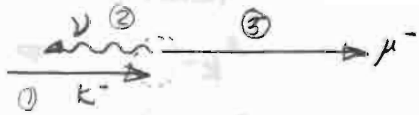

directly forward for maximum momentum transfer

such that maximum momentum is imparted to the μ^- when $\theta_{\mu\text{-}k} = 0$ as shown. The 4-vectors are :

$$P_K = \left(\frac{E_k}{c}, \vec{P}_k \right), \quad P_\nu = \left(\frac{E_\nu}{c}, \vec{P}_\nu \right), \quad P_{\mu^-} = \left(\frac{E_\mu}{c}, \vec{P}_\mu \right)$$

The simplest approach is to find p_ν first, because $E_\nu = p_\nu c$ for a massless particle, and then relate this to p_μ in the CM frame. The invariant inner product, and hence p_μ, are calculated as follows:

$$P_K = P_\nu + P_\mu$$

$$(P_\mu)^2 = (P_K - P_\nu)^2 \quad \text{INVARIANT INNER PRODUCT, } (P_i P^i)$$

$$P_\mu^2 = P_K^2 + P_\nu^2 - 2(P_K P_\nu)$$

$$-m_\mu^2 c^2 = -m_K^2 c^2 - \underset{\to 0}{m_\nu^2 c^2} - 2\left[-\frac{E_K E_\nu}{c \cdot c} + \vec{P}_K \cdot \vec{P}_\nu \right]$$

where $\theta_{K\nu} = \pi$, $\cos\theta_{K\nu} = (-1)$,

and $\frac{E_\nu}{c} = |P_\nu|$,

$$(m_K^2 - m_\mu^2)c^2 = 2\left(\frac{E_K}{c}|\vec{P}_\nu| + |\vec{P}_K||\vec{P}_\nu| \right)$$

$$= 2|\vec{P}_\nu|\left(\frac{E_K}{c} + |\vec{P}_K| \right)$$

$$\Longrightarrow \quad |\vec{P}_\nu| = \frac{(m_K^2 - m_\mu^2)c^2}{2\left(\frac{E_K}{c} + P_K \right)}$$

NOW, IN THE CM FRAME:

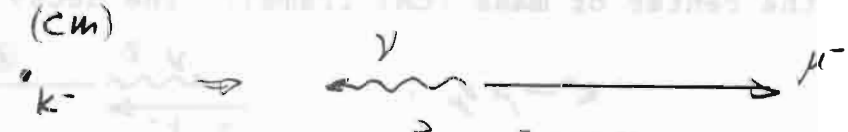

$(\vec{P}_K = 0)$: $\quad \vec{P}_\nu + \vec{P}_\mu = 0$

$$(\therefore) \quad |\vec{P}_\mu| = |\vec{P}_\nu| = \frac{\left[(.494\ \text{GeV}/c^2)^2 - (.1057\ \text{GeV}/c^2)^2 \right] c^2}{2\left[1.579\ \text{GeV}/c + 1.5\ \text{GeV}/c \right]} = \underline{1.47\ \text{GeV}/c}$$

using $E_K = \sqrt{p^2c^2 + m_K^2c^4}$ ...

THUS $|\vec{p}_\mu| = |\vec{p}_\nu| = 1.47$ GeV/c.

Now, this could be missed if the velocity change with respect to the K^- is small, in the absence of a kink in the track. Since relativistically, ~~and~~ the velocity is $v = p(c)^2/E$,

$$V_K = \frac{1.5\ \text{GeV/c} \cdot c^2}{1.577\ \text{GeV}} = .95\ c\ ,$$

$$V_\mu = \frac{1.47\ \text{GeV/c} \cdot c^2}{1.474\ \text{GeV}} = .997\ c$$

So the velocities are comparable. Yet since $m_{\mu^-} \hat{=} \frac{1}{4} m_{k^-}$, the lorentz force $\vec{F} = q\vec{v} \times \vec{B}$ would have a larger effect on the μ^-. This would still reveal the decay by a noticeable change in curvature, even in the absence of a kink. Therefore, I would not consider a small angle K^- decay to be of importance for error considerations.

Some additional points are important in the analysis of the K^- induced reactions (sec. VIII. analysis questions). The value of the K^- mean lifetime was compared with a current Particle Data Table (see ref. 6) and the percent difference was found to be 1.3 %. This published value is based on experiments with K^+ mesons at rest. It is not feasible to measure the K^- lifetime at rest because, in contrast to the K^+ meson, which decays upon coming to rest, the K^- undergoes nuclear capture, so that only decays in flight are observed. (Nickols, 1959)

The mean lifetime was found using the relation $\tau_{lab} = \gamma \tau_{rest}$, which is an equation of time dilation, between two reference frames. This provides confirmation of the relativistic time dilation effects, which are easily visible here, since the velocity of the K^- particles were found to be .95c .

Antiparticles were observed in this experiment. The $\overline{K^0}$ was seen to be produced many times by a K^-p interaction. The K^- has strangeness $S = -1$. In order for strangeness to be conserved in the hadronic process, the $\overline{K^0}$ must have $S = -1$ also. Now, the K^0 is known to have $S = +1$, so it can be inferred that antiparticles have equal and opposite quantum numbers from their corresponding "real" counterparts. This idea can be applied to the K^+. K^+ are never found in any of the reactions, as would be expected, since the K^- has strangeness $S = -1$, and the K^+ has $S = +1$. However since the two K mesons have equal and opposite charge and strangeness, then the K^+ must be the antiparticle to the K^-.

The measured cross section was compared with the accepted value and the percent difference was 2.4 %. The value measured was σ = 56.6 mb = .0566 b = 5.66 fm^2. Using a classical "geometrical" model in which a K^- sees a proton "effective radius", the radius of the proton would be r = (5.66 fm^2/3.14159)^.5 = 1.34 fm .

The total cross section as a function of beam momentum exhibits "bumps", or peaks, which are attributed to the formation of a short lived resonance particle. If it is assumed that the K^- meson and the proton combined to form a resonant particle at this momentum, then the rest mass energy of the resonance would be the energy of the incident

K^- particles : E = ((pc)^2 + m^2c^4)^.5 relativistically, so E = ((1.5 Gev)^2 + (.494 Gev)^2) = 1.579 Gev. So the rest mass energy of the proposed resonance particle is 1.579 Gev.

The resonances would have quantum numbers. Since the resonance peaks occur at specific energy values, this implies that energy is quantized. One quantum number would be energy. Also, the peaks of the cross section versus energy curve would exhibit a width, representative of a small energy variation about some central maximum. So, another quantum number to characterize the resonance would be "width". Also, since additive quantum numbers are conserved in particle reactions, and the initial constituents would have some value of spin, a third quantum number would be spin.

Calculations and Analysis

Photon-proton reactions:

The high energy photon beam used in this experiment was produced at the Stanford Linear Accelerator Center (SLAC), by back scattering a low energy 4.68 eV Nd laser beam directly from a 30 GeV electron beam, generated by the linear accelerator. The resulting back scattered photons carry a large energy due to the relativistic conservation of energy-momentum. Thus, and final energy of the photon beam can easily be calculated using 4-vectors :

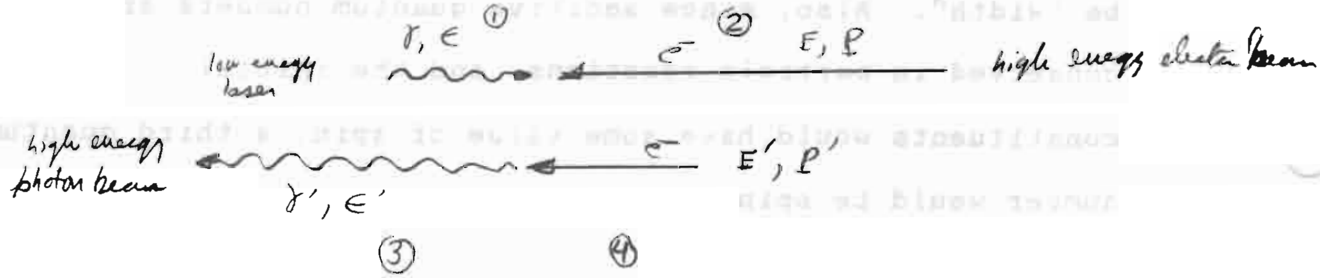

$$p_1^\mu + p_2^\mu = p_3^\mu + p_4^\mu$$ (4-vectors), index "μ".

$$p_1 = \left(\frac{\epsilon}{c}, \vec{P}_\gamma\right), \quad p_2 = \left(\frac{E}{c}, -\vec{P}\right), \quad p_3 = \left(\frac{\epsilon'}{c}, -P_\gamma'\right), \quad p_4 = \left(\frac{E'}{c}, -P'\right)$$

$$p_4^2 = (p_1 + p_2 - p_3)^2$$ Invariant inner product.

$$p_4^2 = p_1^2 + p_2^2 + p_3^2 + 2(p_1 p_2 - p_1 p_3 - p_2 p_3)$$

$$-m_e^2 c^2 = \underset{(m_\gamma = 0)}{-m_\gamma^2 c^2} - m_e^2 c^2 - m_\gamma^2 c^2 + 2(p_1 p_2 - p_1 p_3 - p_2 p_3)$$

$$0 = (p_1 p_2 - p_1 p_3 - p_2 p_3)$$

$$= \left(-\left(\frac{\epsilon}{c}\frac{E}{c}\right) + \vec{p}_1 \cdot \vec{p}_2 - \left(-\frac{\epsilon}{c}\frac{\epsilon'}{c} + \vec{p}_1 \cdot \vec{p}_3\right) - \left[-\left(\frac{\epsilon'}{c}\frac{E}{c}\right)\right.\right.$$

$$0 = -\frac{\epsilon}{c}\frac{E}{c} - |p_1||p_2| + \frac{\epsilon}{c}\frac{\epsilon'}{c} + |p_1||p_3| + \frac{E}{c}\frac{\epsilon'}{c} - |p_2||p_3|$$

For photons: $\frac{\epsilon}{c} = p_1$, $p_3 = \frac{\epsilon'}{c}$;

$$= -\frac{\epsilon}{c}\frac{E}{c} - \frac{\epsilon}{c}P + \frac{\epsilon}{c}\frac{\epsilon'}{c} + \frac{\epsilon}{c}\frac{\epsilon'}{c} + \frac{E}{c}\frac{\epsilon'}{c} - P\frac{\epsilon'}{c}$$

$$= -\epsilon E - c\epsilon P + \epsilon\epsilon' + \epsilon\epsilon' + E\epsilon' - cP\epsilon'$$

$$= \epsilon'(2\epsilon + E - cP) - \epsilon E - c\epsilon P$$

$$\epsilon'(2\epsilon + E - cP) = \epsilon E + c\epsilon P$$

$$\therefore \quad \epsilon' = \frac{\epsilon(E + cP)}{2\epsilon + E - cP} = \frac{\epsilon\left(E + \sqrt{E^2 - m_e^2c^4}\right)}{2\epsilon + E - \sqrt{E^2 - m_e^2c^4}}$$

Now $\epsilon = 4.68\,eV = 7.488\times10^{-19}\,J$, $E = 30\,GeV = 4.8\times10^{-9}\,J$, $m_e = 9.11\times10^{-31}\,kg$, $c = 3\times10^{8}\,m/s$,

$$\epsilon' = \frac{7.488\times10^{-19}\,J\left((4.8\times10^{-9})^2 - \sqrt{(4.8\times10^{-9})^2 - (9.11\times10^{-31}(3\times10^8)^2)^2}\right)}{2(7.488\times10^{-19}) + 4.8\times10^{-9} - \sqrt{(4.8\times10^{-9})^2 - ((9.11\times10^{-31})(3\times10^8)^2)^2}}$$

$$= 3.267\times10^{-9}\,J = \boxed{20.5\ GeV}$$ energy of back-scattered photon bea

Also, (prob. 4.2), 4-vectors can be used to prove that pair production cannot occur in a vacuum. This is because a proton (or other nucleus) must be in the vicinity to take up the required amount of energy-momentum of the electron and positron produced.

$$\gamma \rightarrow e^+e^-$$

$$(P_\gamma)^2 = (P_+ + P_-)^2$$

$$-\underset{0}{m_\gamma^2c^2} = -m_{e^+}^2c^2 - m_{e^-}^2c^2 + 2\left[-\left(\frac{E_+E_-}{c^2}\right) + \underset{0}{\vec{p}_+}\cdot\vec{p}_-\right]$$

- evaluate in CM frame of e^+; $\vec{P}_+ = 0$

$$0 = -2m_e^2c^2 - 2\,\frac{E_+E_-}{c^2} \quad ; (m_{e^+} = m_{e^-});$$

$E_+ = E_- = m_ec^2$, at rest in CM frame,

$$0 = -2m_e^2c^2 - 2\frac{m_e^2c^4}{c^2}$$

$$0 = -2m_e^2c^2 - 2m_e^2c^2$$

$$0 \neq 4m_e^2c^2$$

$\Rightarrow$ $\gamma \to e^+e^-$ NOT POSSIBLE, (IN VACUUM)

(∴) $\boxed{\text{PAIR PRODUCTION CANNOT OCCUR IN VACUUM.}}$

HOWEVER, $\gamma p \to p e^+ e^-$ IS POSSIBLE, BECAUSE THE p BALANCES ENERGY-MOMENTUM:

$$\gamma p \to p e^+ e^-$$

$$(p_1 + p_2)^2 = (p_3 + p_4 + p_5)^2$$

$$-\underset{0}{m_\gamma^2}c^2 - m_2^2c^2 + 2E_1 m_2 c = -M^2c^2 \quad , M = m_3 + m_4 + m_5,$$

$$-m_2^2c^2 - 2E_\gamma m_2 = -(m_p + m_{e^+} + m_{e^-})^2 c^2$$

$$= -[m_p^2 + 4m_p m_e + 4m_e^2]c^2$$

$$m_2^2c^2 - 2E_\gamma m_p = (m_p^2 + 4m_p m_e + 4m_e^2)c^2$$

$$2E_\gamma m_2 = (\cancel{m_p^2c^2} + 4m_p m_e + 4m_e^2) - \cancel{m_p^2c^2}$$

$$E_\gamma m_p = 2(m_p m_e + m_e^2)c^2$$

$$E_\gamma = \frac{2(m_p m_e + m_e^2)c^2}{m_p}$$

"THRESHOLD ENERGY FOR PAIR PRODUCT IN PRESENCE OF P

$$E_\gamma = 2m_ec^2 + \left(\frac{m_e^{\cancel{2}}}{\cancel{m_p}}\right)c^2$$

$$\left(\frac{m_e^2}{m_p}\right) \ll m_e$$

(∴) E_γ ______

products, e^+ and e^-.

So : $\sigma = \dfrac{-\ln\left[1-\frac{268}{4450}\right]\cdot 1}{(6.022\times10^{23})(.06\ \mathrm{g/cm^3})(30.48\ \mathrm{cm})} = 5.64\times10^{-26}\ \mathrm{cm}^2$

Now cross section units are stated in 'barns', b, in the SI system; 1 b = 10^-24 cm^2 = 100 fm^2 . So σ = 56.4 mb.

This value could be low due to systematic scanning error, for the cases when $K^-p \to pK^-$ scattering occurs at very small angles. To correct for this (optional problem 1), the differential cross section correction for small angles can be employed:

$$\frac{d\sigma}{dt} \doteq \frac{70\ \mathrm{mb}}{(\mathrm{GeV/c})^2}$$

where t is the square of the 4-momentum transfer. At small angles, this becomes t = (p θ)^2, which correctly produces the units above in 1/(Gev/c)^2, and 'p' is the beam momentum of 1.5 Gev/c. I have found it very difficult to spot scattering at $\theta < 2^\circ$; 2° = .035 radians, so:

$$\sigma_{\mathrm{CORRECTION}} \doteq \frac{70\ \mathrm{mb}}{(\mathrm{GeV/c})^2}\left[1.5\ \mathrm{GeV/c}\right]^2(.035\ \mathrm{radians})^2 = .20\ \mathrm{mb}$$

This correction must be added to the preliminary value, because missing $K^-p \to pK^-$ events lowers the value of σ_{tot}. So the corrected crossection is: σ = 56.4 mb + .20 mb = 56.6 mb

Again, the error is dominated by random counting errors, so $\Delta n = \sqrt{n}$, as before, $\dfrac{\Delta\sigma}{\sigma} = \dfrac{\Delta n}{n} = \dfrac{\sqrt{n}}{n} = \dfrac{\sqrt{268}}{268}$,

So.
$$\Delta\sigma = 56.6\ mb\left(\frac{\sqrt{268}}{268}\right) = 3.50\ mb$$

The final value is: $\boxed{\sigma = 56.6 \pm 3.5 \text{ mb}}$ (at 1.5 Gev/c)

The accepted value[4] of σ at 1.5 Gev/c beam momentum is

σ = 58.0 mb (R.L. Cool, 1966). The percent difference is

$\frac{(58.0 - 56.6)(100\%)}{(58.0)} = 2.4\%$.

The K^- lifetime is found from the differential equation expressing K^- beam attenuation, as above, however, this time the contribution due to decays in flight is considered:

$$\frac{dN_D}{dx} = -N\left(\frac{1}{\beta\gamma c\tau}\right) \longrightarrow \ln(N/N_0) = \frac{-\Delta x_{FIDUCIAL}}{\beta\gamma c\tau},$$

$$\tau = \frac{-\Delta x_{FIDUCIAL}}{\ln(N/N_0)\gamma\beta c}$$

AS BEFORE, $N_0 - N_{eff} = \Delta N_D$ = total decays observed (117)

$$N - N_0 = -\Delta N_D$$

$$\frac{N}{N_0} = \left[1 - \frac{\Delta N_D}{N_0}\right] = \left[1 - \frac{117}{4450}\right]$$

USING $\beta\gamma = \frac{P}{mc} = \frac{(1.5\ GeV/c)}{(.494\ GeV/c^2)c} = 3.036$ [dimensionless]

$$\tau = \frac{-(.3048\ m)}{\ln\left[1 - \frac{117}{4450}\right](3.036)(3\times10^8\ m/s)} = 1.256\times10^{-8}\ \sec$$

Relevant contributions to error in the mean lifetime are due to $\Delta m_{K^-} = \pm 2$ Mev/c^2[1], and random counting with $\Delta n = \sqrt{n}$.

References

1. D.H. Perkins, "Introduction to High Energy Physics", 2nd edition (Addison-Wesley, 1982).

2. B.R. Martin and G. Shaw, "Particle Physics", John Wiley & Sons, 1992.

3. D. Griffiths, "Introduction to Elementary Particles", Wiley, 1987.

4. R.L. Cool et al, "K^-p Total Cross Sections from 1 to 2.5 Gev/c", Phys. Rev. Letters 16, 1228 (1966).

5. S. A. Wolbers, "Inclusive Photoproduction of Strange Baryons at 20 GeV", Ph.D. thesis, UC Berkeley, 1984.

6. "Review of Particle Properties", Phys. Rev. D50, 1173 (1994).

APPENDIX

① SKETCHES

② RAW DATA

SKETCHES

γ, e^- collision
FRAME # 671

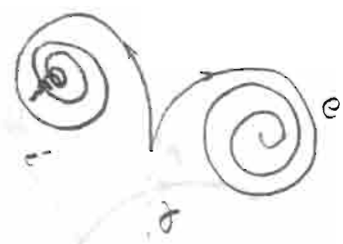

low energy pair production
$\gamma p \to (p) e^+ e^-$
FRAME # 705

E.M. Shower.
FRAME # 708

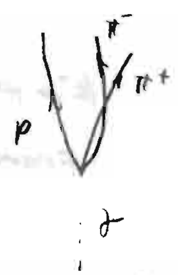

$\gamma \to p \pi^+ \pi^-$
3 prong event
FRAME # 694

$\gamma p \to (p) \pi^+ \pi^- \pi^+ \pi^-$
5 prong
FRAME # 706

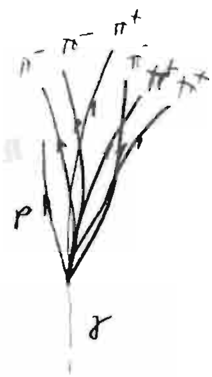

7 prong FRAME # 72[illegible]

3 prong with Vee
FRAME # 876

5 prong w/vee
FRAME # 843

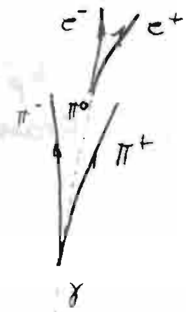

2 prong w/vee
FRAME # 799

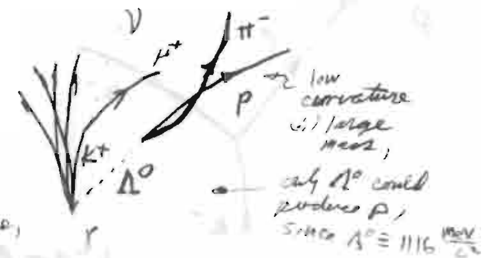

FRAME # 588

FRAME # 95-

SKETCHES

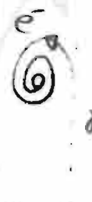

γ, e⁻ collision
FRAME # 671

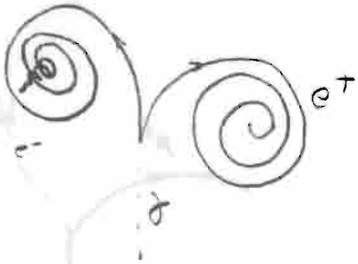

low energy pair production
$\gamma p \to (p)\, e^+ e^-$
FRAME # 705

E.M. Shower.
FRAME # 708

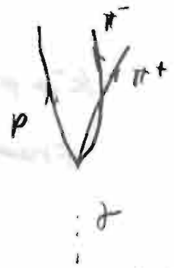

$\gamma \to p \pi^+ \pi^-$
3 prong event
FRAME # 694

$\gamma p \to (p)\, \pi^+ \pi^- \pi^+ \pi^-$
5 prong
FRAME # 706

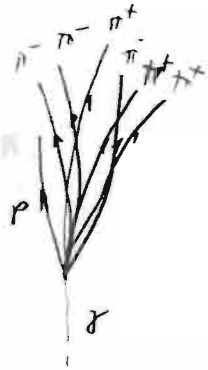

7 prong
FRAME # 722

3 prong with vee
FRAME # 876

5 prong w/vee
FRAME # 843

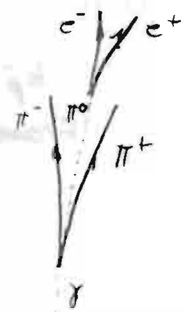

2 prong w/vee
FRAME # 799

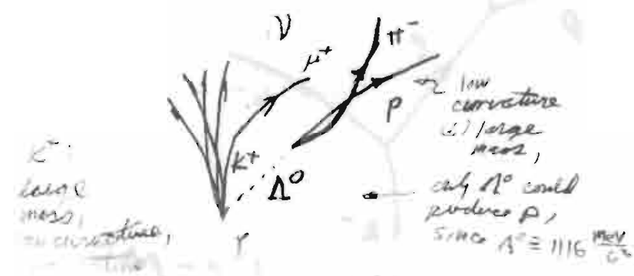

FRAME # 588

FRAME # 95-

DATA

4-9-96

FRAME #	REACTION
664	$K^- \to \mu^- \nu_\mu$ decay
665	$K^- \to \mu^- \nu_\mu$ decay $K^- p \to p K^-$ elastic, 2 prong
666	$K^- p \to p K^-$, $K^- p \to p K^-$ elastic, elastic
668	$K^- p \to p K^-$; $K^- p \to p K^-$ elastic, elastic, 2 prong
669	$K^- \to \mu^- \nu_\mu$ decay
670 (8)	$K^- p \to p K^-$ elastic, 2 prong $K^- p \to p K^-$ elastic, 2 prong
671	$K^- p \to n \bar{K}^0$ disappears inelastic, (no charged products)
673	$\boxed{K^- \to \pi^- \pi^- \pi^+}$ τ mode decay $K^- p \to p K^-$ elastic, 2 prong $K^- p \to p K^-$ elastic, 2 prong
674	$K^- \to \mu^- \nu_\mu$ decay $K^- \to \mu^- \nu_\mu$ decay
676	$K^- p \to \pi^+ \pi^- \Lambda^0$, $\Lambda^0 \to p \pi^-$ inelastic, 2 prong w/ vee
677	$K^- \to \mu^- \nu_\mu$ decay
678	$K^- \to \mu^- \nu_\mu$ decay $K^- p \to p K^-$ elastic, 2 prong $K^- p \to p K^-$ elastic, 2 prong
679	$K^- p \to p K^-$ elastic, 2 prong $K^- p \to p K^-$ elastic
680 (9)	$K^- p \to n \bar{K}^0$ disappears
681	$K^- p \to p K^-$ elastic, 2 prongs $K^- p \to p K^-$ elastic " $K^- p \to n \bar{K}^0$ inelastic, disappears

FRAME #	REACTION
682	$K^- p \to p K^-$ elastic, 2 pr. $K^- \to \mu^- \nu_\mu$ decay
686	$K^- p \to p K^-$ elastic $K^- p \to p K^-$ elastic
687	$K^- \to \mu^- \nu_\mu$ decay $K^- p \to p K^-$ elastic, 2 pr.
688	$K^- \to \mu^- \nu_\mu$ decay $K^- p \to p K^-$ elastic $K^- p \to p K^-$; $K^- p \to p K^-$ - elastic
689	$K^- p \to p K^-$; $K^- p \to p K^-$ elastic
690 (10)	$K^- p \to p K^-$ elastic $K^- p \to \pi^+ \pi^- \Lambda^0$, $\Lambda^0 \to p \pi^-$ inelastic, 2 prong w/ vee
691	$K^- p \to p K^-$ elastic, 2 prong $K^- \to \mu^- \nu_\mu$ decay
693	$K^- p \to \pi^+ \pi^- \Lambda^0$, $\Lambda^0 \to \pi^- p$ inelastic, 2 prongs w/ vee
694	$K^- p \to K^- p$ elastic, 2 pr. $K^- \to \mu^- \nu_\mu$ decay $\boxed{K^- \to \pi^+ \pi^- \pi^-}$ τ decay $K^- p \to p K^-$ elastic, 2 prong
695	$K^- p \to p K^-$, $K^- p \to p K^-$ elastic, elastic, 2 prong
697	$K^- p \to p K^-$ elastic $K^- \to \mu^- \nu_\mu$ decay $K^- \to \mu^- \nu_\mu$ decay $K^- p \to p K^-$ elastic, 2 prongs
702 (12)	$K^- p \to p K^-$ elastic 2 prongs $K^- p \to p K^-$ elastic

DATA

4-9-96

FRAME #	REACTION
703	$K^- \to \mu^- \nu_\mu$ decay $K^-p \to pK^-$ elastic, 2 prong
704	$K^-p \to pK^-$ elastic, 2 pr $K^-p \to pK^-$ elastic "
706	$K^-p \to pK^-$ elastic, 2
708	$K^-p \to pK^-$ elastic, 2
709	$K^-p \to pK^-$ elastic, 2 $K^- \to \mu^- \nu_\mu$ decay $K^-p \to pK^-$ elastic
710 (8)	$K^- \to \mu^- \nu_\mu$ decay $K^-p \to pK^-$ elastic, 2
712	$K^- \to \mu^- \nu_\mu$ decay $K^-p \to pK^-$ elastic, 2
713	$K^-p \to pK^-$ elastic, 2 $K^-p \to pK^-$ elastic, 2
714	$K^-p \to pK^-$ elastic, 2 $K^-p \to pK^-$ " $K^-p \to pK^-$ "
718 (7)	$K^-p \to pK^-$, $\hookrightarrow pp$ elastic, elastic, 2 pr.
725	$K^-p \to pK^-$ elastic, 2 prong
727 (7)	$K^-p \to pK^-$ elastic, 2 pr. $K^-p \to pK^-$ elastic "
737	$K^-p \to pK^-$ elastic, 2 prong
741 (9)	$K^-p \to pK^-$ elastic, 2 prong $K^- \to \mu^- \nu_\mu$ decay
742	$K^-p \to$ elastic, 2 pr.

FRAME #	REACTION
744	$K^-p \to pK^-$ elastic, 2 pr. $K^-p \to pK^-$ elastic "
751 (10)	$K^-p \to pK^-$ elastic
755	$K^-p \to pK^-$ elastic, 2 pr $K^-p \to pK^-$ elastic, "
758	$K^- \to \mu^- \nu_\mu$ decay
761 (9)	$K^- \to \mu^- \nu_\mu$ decay $K^-p \to pK^-$ elastic
764	$K^-p \to pK^-$ elastic
766	$K^- \to \mu^- \nu_\mu$ decay $K^-p \to pK^-$ elastic, 2
768	$K^- \to \mu^- \nu_\mu$ decay $K^-p \to pK^-$ elastic, 2
769	$K^-p \to pK^-$ elastic, 2 prong
771 (8)	$K^-p \to \pi^+\pi^-\Lambda^0$, $\hookrightarrow p\pi^-$ inelastic, 2 prong w/vee
780 (10)	$K^-p \to pK^-$ elastic, 2 prong $K^-p \to pK^-$ " , $K^-p \to pK^-$ " , "
782	$K^-p \to pK^-$ elastic, 2 $K^- \to \mu^- \nu_\mu$ decay
783	$K^- \to \mu^- \nu_\mu$ decay $K^-p \to pK^-$ elastic, 2 prong
784	$K^-p \to pK^-$ elastic, 2 pr $K^-p \to nK^0$ inelastic, 0 pr
786	$K^-p \to pK^-$, $K^-p \to pK^-$ elastic, elastic

DATA

4-12-96

FRAME #	REACTION
789	$K^- \to \mu^- \nu_\mu$ decay $K^- p \to p K^-$ elastic, 2 prong
790 (8)	$K^- \to \mu^- \nu_\mu$ decay $K^- p \to p K^-$ elastic, 2 prong
791	$K^- p \to p K^-$ elastic, 2 prong $K^- p \to p K^-$ elastic, 2 prong
792	$K^- p \to p K^-$ elastic, 2
794	$K^- p \to p K^-$ elastic, 2
795	$K^- p \to p K^-$ elastic, 2 $K^- p \to n \bar{K}^0$ ~~disappears~~ inelastic $K^- p \to p K^-$ elastic, 2
798	$K^- \to \mu^- \nu_\mu$ decay $K^- p \to p K^-$ elastic, 2
800 (7)	$K^- \to \mu^- \nu_\mu$ decay $K^- p \to p K^-$ elastic, 2
801	$K^- p \to n \bar{K}^0$ inelastic, 0
806	$K^- p \to p K^-$ elastic, 2
807	$K^- \to \mu^- \nu_\mu$ decay
808	$K^- \to \mu^- \nu_\mu$ decay
810 (9)	$K^- p \to p K^-$ elastic, 2 $K^- p \to p K^-$ elastic, 2 $K^- p \to p K^-$ elastic, 2
814	$K^- \to \mu^- \nu_\mu$ decay $K^- p \to p K^-$ elastic, 2
817	$\boxed{K^- \to \pi^+ \pi^- \pi^-}$ τ mode decay $K^- p \to p K^-$ elastic, 2 prong $K^- p \to p K^-$ elastic, 2 prong

FRAME #	REACTION
818	$K^- p \to p K^-$ elastic, 2 $K^- p \to p K^-$ elastic, 2
819	$K^- \to \mu^- \nu_\mu$ decay $K^- p \to n \bar{K}^0$ inelastic $K^- p \to p K^-$ elastic, 2 prong
821 (9)	$K^- \to \mu^- \nu_\mu$ decay $K^- p \to p K^-$ elastic, 2 prong $K^- p \to p K^-$ elastic, 2 $K^- p \to p K^-$ elastic, 2 $\quad \hookrightarrow pp$
822	$K^- \to \mu^- \nu_\mu$ decay $K^- p \to p K^-$ elastic, 2
823	$K^- \to \mu^- \nu_\mu$ decay $K^- p \to p K^-$ elastic, 2
827	$K^- \to \mu^- \nu_\mu$ decay $K^- \to \mu^- \nu_\mu$ decay $K^- p \to p K^-$ elastic, 2 $K^- p \to p K^-$ elastic, 2
828	$K^- \to \mu^- \nu_\mu$ decay $K^- p \to p K^-$ elastic
832 (10)	$K^- p \to \pi^+ \pi^- \Lambda^0$, $\Lambda^0 \to p \pi^-$ inelastic, 2 prong w/ vee
833	$K^- p \to p K^-$ elastic, 2 $K^- p \to p K^-$ elastic, 2
835	$K^- p \to p K^-$ elastic, 2
837 (10)	$K^- \to \mu^- \nu_\mu$ decay $K^- p \to p K^-$ elastic, 2
846	$K^- p \to p K^-$ elastic, 2
849 (9)	$K^- p \to p K^-$ elastic, 2 $K^- \to \mu^- \nu_\mu$ decay

DATA

4-12-96

FRAME #	REACTION	FRAME #	REACTION
789	$K^- \to \mu^- \nu_\mu$ decay $K^- p \to p K^-$ elastic, 2 prong	818	$K^- p \to p K^-$ elastic, 2 $K^- p \to p K^-$ elastic, 2
790 (8)	$K^- \to \mu^- \nu_\mu$ decay $K^- p \to p K^-$ elastic, 2 pro.	819	$K^- \to \mu^- \nu_\mu$ decay $K^- p \to n \bar{K}^0$ inelastic $K^- p \to p K^-$ elastic, 2 pr.
791	$K^- p \to p K^-$ elastic, 2 prong $K^- p \to p K^-$ elastic, 2 prong	821 (9)	$K^- \to \mu^- \nu_\mu$ decay $K^- p \to p K^-$ elastic, 2 pr. $K^- p \to p K^-$ elastic, 2 $K^- p \to p K^-$ elastic, 2 $\hookrightarrow pp$
792	$K^- p \to p K^-$ elastic, 2	822	$K^- \to \mu^- \nu_\mu$ decay $K^- p \to p K^-$ elastic, 2
794	$K^- p \to p K^-$ elastic, 2	823	$K^- \to \mu^- \nu_\mu$ decay $K^- p \to p K^-$ elastic, 2
795	$K^- p \to p K^-$ elastic, 2 $K^- p \to n \bar{K}^0$ ~~disappears~~ inelastic $K^- p \to p K^-$ elastic, 2	827	$K^- \to \mu^- \nu_\mu$ decay $K^- \to \mu^- \nu_\mu$ decay $K^- p \to p K^-$ elastic, 2 $K^- p \to p K^-$ elastic, 2
798	$K^- \to \mu^- \nu_\mu$ decay $K^- p \to p K^-$ elastic, 2	828	$K^- \to \mu^- \nu_\mu$ decay $K^- p \to p K^-$ elastic
800 (7)	$K^- \to \mu^- \nu_\mu$ decay $K^- p \to p K^-$ elastic, 2	832 (10)	$K^- p \to \pi^+ \pi^- \Lambda^0$ $\hookrightarrow p \pi^-$ inelastic, 2 prong v/vee
801	$K^- p \to n \bar{K}^0$ inelastic, 0	833	$K^- p \to p K^-$ elastic, 2 $K^- p \to p K^-$ elastic, 2
806	$K^- p \to p K^-$ elastic, 2	835	$K^- p \to p K^-$ elastic, 2
807	$K^- \to \mu^- \nu_\mu$ decay	837 (10)	$K^- \to \mu^- \nu_\mu$ decay $K^- p \to p K^-$ elastic, 2
808	$K^- \to \mu^- \nu_\mu$ decay	846	$K^- p \to p K^-$ elastic, 2
810 (9)	$K^- p \to p K^-$ elastic, 2 $K^- p \to p K^-$ elastic, 2 $K^- p \to p K^-$ elastic, 2	849 (9)	$K^- p \to p K^-$ elastic, 2 $K^- \to \mu^- \nu_\mu$ decay
814	$K^- \to \mu^- \nu_\mu$ decay $K^- p \to p K^-$ elastic, 2		
817	$\boxed{K^- \to \pi^+ \pi^- \pi^-}$ τ mode decay $K^- p \to p K^-$ elastic, 2 prong $K^- p \to p K^-$ elastic, 2 prong		

DATA

FRAME #	REACTION
902	$K^- \to \mu^- \nu_\mu$ decay $K^-p \to pK^-$ elastic, 2 prong
903	$K^-p \to pK^-$ elastic, 2 $K^-p \to pK^-$ elastic, 2
905	$K^-p \to pK^-$ elastic $K^-p \to pK^-$ elastic
908	$K^- \to \mu^- \nu_\mu$ decay $K^-p \to pK^-$ elastic, 2
909	$K^- \to \mu^- \nu_\mu$ decay $K^-p \to pK^-$ elastic, 2
910 (9)	$K^-p \to pK^-$ elastic, 2 prong
911	$K^-p \to pK^-$ elastic, 2 $K^-p \to pK^-$ elastic, 2
914	$\boxed{K^- \to \pi^-\pi^-\pi^+}$ τ mode decay $K^-p \to pK^-$ elastic, 2 prong
915	$K^-p \to pK^-$ elastic, 2 $K^-p \to pK^-$ elastic, 2
916	$K^-p \to pK^-$ elastic, 2
919	$K^-p \to pK^-$ elastic, 2
920 (8)	$K^-p \to p\pi^-\bar{K}^0$, $\bar{K}^0 \to \pi^+\pi^-\nu$ inelastic, 2 prong w/vee
921	$K^-p \to pK^-$ elastic, 2
922	$K^- \to \mu^- \nu_\mu$ decay $K^-p \to pK^-$ elastic, 2
924	$K^-p \to \pi^-\pi^+\pi^-\Sigma^+$, $\Sigma^+ \to p\pi^0$ inelastic, 4 prong $\tau(\Sigma^+) \sim 10^{-10}$ seconds; p large mass; track curvature is small.

FRAME #	REACTION
925	$K^- \to \mu^- \nu_\mu$ decay $K^-p \to pK^-$ elastic
929	$K^-p \to pK^-$ elastic, 2
931 (9)	$K^- \to \mu^- \nu_\mu$ decay $K^-p \to pK^-$ elastic, 2
932	$K^- \to \mu^- \nu_\mu$ decay $K^-p \to pK^-$ elastic, 2
933	$K^- \to \mu^- \nu_\mu$ decay $K^-p \to pK^-$ elastic, 2 pr.
935	$K^- \to \mu^- \nu_\mu$ decay
936	$K^- \to \mu^- \nu_\mu$ decay $K^-p \to pK^-$ elastic, 2 pr.
938	$K^-p \to pK^-$ elastic, 2
939	$K^-p \to \pi^+\pi^-\Lambda^0$, $\Lambda^0 \to p\pi^-$ inelastic 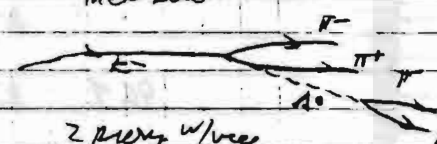 2 prong w/vee
940 (8)	$K^-p \to pK^-$ elastic, 2 $K^-p \to pK^-$ elastic, 2
943	$K^-p \to pK^-$ elastic
944	$K^- \to \mu^- \nu_\mu$ decay $K^-p \to pK^-$ elastic, 2 $K^-p \to pK^-$ elastic, 2
945	$K^-p \to pK^-$ elastic, 2
947	$K^- \to \mu^- \nu_\mu$ decay $K^-p \to pK^-$ elastic, 2 prong.

DATA

FRAME #	REACTION
948	$K^-p \to pK^-$ elastic, 2
953 (10)	$K^-p \to pK^-$ elastic, 2 $K^-p \to pK^-$ elastic 2 $K^-p \to pK^-$ elastic, 2
954	$K^-p \to pK^-$ elastic, 2 $K^-p \to pK^-$ elastic, 2
957	$K^-p \to pK^-$ elastic, 2
958	$K^- \to \mu^- \nu_\mu$ decay
961 (10)	$K^-p \to \pi^+\pi^-\Lambda^0$, $\Lambda^0 \to p\pi^-$ inelastic, 2 prong w/vee
963	$K^-p \to nK^0$ inelastic, 0, $K^0 \to \pi^+\pi^-$, vee
964	$K^- \to \mu^- \nu_\mu$ decay
965	$K^- \to \mu^- \nu_\mu$ decay $K^-p \to pK^-$ elastic, 2 prong
967	$K^-p \to pK^-$ elastic, 2
970 (9)	$K^- \to \mu^- \nu_\mu$ decay
972	$K^- \to \mu^- \nu_\mu$ decay
974	$K^-p \to pK^-$ elastic, 2
976	$K^-p \to \pi^+\pi^-\Lambda^0$, $\Lambda^0 \to p\pi^-$ inelastic, 2 prong w/vee
977	$K^- \to \mu^- \nu_\mu$ decay
978	$K^-p \to pK^-$ elastic, 2
980 (8)	$K^-p \to nK^0$, $K^0 \to \pi^+\pi^-$ inelastic, 2 prong w/vee
983	$K^-p \to pK^-$ elastic, 2 pr.
984	$K^- \to \mu^- \nu_\mu$ decay $K^-p \to pK^-$ elastic, 2 pr.
986	$K^-p \to \pi^+\pi^-\Lambda^0$, $\Lambda^0 \to p\pi^-$ inelastic, 2 prong w/vee
987	$K^-p \to pK^-$ elastic, 2 prong
988	$K^-p \to pK^-$ elastic, 2 $K^-p \to pK^-$ elastic, 2
991 (7)	$K^- \to \mu^- \nu_\mu$ decay
992	$K^- \to \mu^- \nu_\mu$ decay
995	$K^- \to \pi^+\pi^-\Lambda^0$, $\Lambda^0 \to p\pi^-$ inelastic, 2 prong w/vee
996	$K^- \to \mu^- \nu_\mu$ decay
997	$K^- \to \mu^- \nu_\mu$ decay
1000 (8)	$K^-p \to pK^-$ elastic, 2 pr.

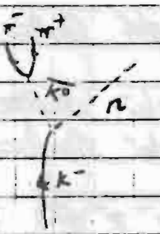

(# good beam tracks)

total $K^- \to \pi^+\pi^+\pi^-$ decays = 7

total $K^-p \to X$ interactions = 268

total $K^- \to X$ decays = 117

average # of good beam tracks $= \frac{\Sigma \#}{500} = 8.90$

DATA 9-16-96

PHOTON-PROTON REACTIONS — select frames (480-980)

40" bubble chamber (SLAC) (BC 72/73)

classify: electromagnetic interactions as Em
hadronic photoproduction as h

prongs given as a number, ie — 2, 3, etc.

FRAME #	REACTION (prong #, Em, or h)	FRAME #	REACTION
480	2, Em	545	2-Em
483	2, Em, 3-h	546	5, h
486	2, Em	547	2-Em
491	2, 2, Em	551	2-Em
494	2 Em	552	2-Em
497	3-Em	555	2-Em
502	5-h	558	2-Em
503	3 Em	565	3, 3, Em
506	3-Em	566	3, Em
507	2-Em	567	2, 2, Em
508	2-Em	569	2, Em
510	2-Em	571	7-h
514	2-Em	572	2-Em
524	2-Em	575	2- pair production, Em
525	2-Em	579	7-h
533	2-Em	588	7-h ($\Sigma S = 0$)
537	2-Em		
544	3-Em		

$\gamma p \to (p)\pi^+\pi^-\pi^-K^+\Lambda^0$

$\boxed{\begin{array}{l} K^+ \to \mu^+\nu_\mu \\ \Lambda^0 \to p\pi^- \end{array}}$

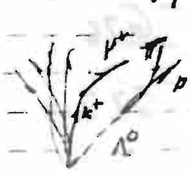

$S = -1 + 1 = 0$ ✓

FRAME #	REACTION	FRAME #	REACTION
590	2-Elm	629	3,2, Elm
592	2-Elm	630	2,2, Elm
593	2-Elm	634	2, Elm
600	2-Elm	635	2, Elm
602	5-h	636	2,2, Elm
603	2-Elm	637	2, Elm
604	2-Elm	638	2, Elm
606	3-Elm	639	3, Elm
607	3-Elm	640	2, Elm
608	2-Elm	641	2, Elm
613	2 Elm	642	3-Elm
614	2-Elm	644	2,2, Elm
617	2-Elm	646	2, Elm
618	2,3, Elm	649	2, Elm
619	2, Elm	650	2, Elm
620	2, Elm	651	7, -h
621	2,2, Elm	653	2,2, Elm
623	2, Elm	655	2,2, Elm
624	3-Elm	656	2,2, Elm
625	2-Elm	658	2 Elm
626	2-Elm	659	2 Elm
627	2-Elm	660	2,2,2 Elm
[illegible]	2 Elm, 5 h	[illegible]	2 Elm

FRAME #	REACTION	FRAME #	REACTION
662	2, Em	692	2-Em
663	$\gamma p \to p\pi^+ K^+ \Lambda^0$, $\Lambda^0 \to p^+\pi^-$	693	2,2, Em
	hadronic, strange particle production	694	3-h
	$\Sigma S = +1-1 = 0$ ✓	695	7-h
664	2-Em	697	3-Em
665	11-h 2-Em	698	2,2,2,2 Em shower
667	7-h	700	2-Em
		701	2,2, Em
668	3-Em	704	7-h
671	2-Em	705	2-Em
672	2-Em	706	5-h
673	2 Em	708	2,2,2,2,2 (Em shower)
674	2,2, Em	711	2,2 Em
675	9-h, 2,2 Em	712	2, Em
678	2,2, Em	717	2,2, Em
6[illegible]	2,2, Em	718	3-Em
680	2-Em	719	2,2, Em
681	2-Em	720	2, Em
684	2,2, Em	722	2-Em
686	2-Em	724	3,2,2 Em
687	7-h	726	2, 7-h
6[illegible]	2-Em	727	2,2, Em ; 3-h
69[illegible]	2-Em	728	7-h

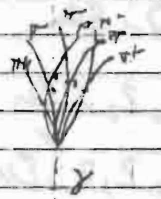

FRAME #	REACTION	FRAME #	REACTION
729	2,2 Elu	774	5-h, 2-Elu
730	2,2, Elu	776	2-Elu
731	2, Elu	778	2-Elu
733	2, Elu	779	3-h
735	2, Elu	781	5-h
737	2-Elu	785	2-Elu
738	2,2, Elu	786	2-Elu
745	2,2,2,2 (Elu shower)	788	2-Elu
748	2,2,2 Elu	789	2-Elu
749	2-Elu, 3-h	791	2-Elu
750	2-Elu	795	2-Elu
752	2,2,2 Elu	796	5-h Elu/prong with 2 vee
756	2,2 Elu		
758	2-Elu	799	2 w/vee-h
760	5-h		
762	2-Elu		
765	5-h	801	2,2,2 Elu
767	2-Elu	804	2 w/vee / h
768	5-h	806	2,2,2 Elu
769	2-Elu	807	2,2,2 Elu
770	5-h, 2-Elu	810	2 Elu
771	5-h	811	2 Elu
772	2, 2, Elu	814	2. Elu

DATA

4-8-96

K^- induced reactions : frames (500 - 1000) selected ; 25" Bubble Chamber

FRAME #	REACTION
503 #K^- = 10	$K^-p \to K^-p$ elastic, 2 prong
507	$K^-p \to \pi^+\pi^-\Lambda^0$, $\Lambda \to p\pi^-$ inelastic, 2 prong w/vee
508	$K^- \to \mu^-\nu_\mu$, $K^-p \to pK^-$ decay in flight, elastic, 2 pr.
510 (8)	$K^-p \to pK^-$, $K^- \to \mu^-\nu_\mu$ elastic, 2 pr; decay,
511	$K^-p \to pK^-$, $K^-p \to pK^-$ elastic, 2 prong
517	$K^-p \to pK^-$, $K^-p \to pK^-$
521 (11)	$K^- \to \mu^-\nu_\mu$, $\boxed{K^- \to \pi^+\pi^-\pi^-}$ decay, decay, 3 prong
522	$K^-p \to \pi^+\pi^-$, $\pi^+ \to \mu^+\nu_\mu$ inelastic, 2 prong
524	$K^-p \to pK^-$ elastic, 2 prong
525	$K^- \to \mu^-\nu_\mu$ decay in flight
528	$K^-p \to pK^-$, $K^-p \to pK^-$ elastic, elastic
530 (7)	$K^- \to \mu^-\nu_\mu$, $K^-p \to pK^-$ decay, elastic, 2 pr.
532	$K^-p \to \pi^+\pi^-\Lambda^0$, $\Lambda \to p\pi^-$ inelastic; decay of Λ^0. (2 prong w/vee)
533	$K^-p \to pK^-$, $K^-p \to pK^-$ elastic, 2 prong
534	$K^-p \to pK^-$, $K^-p \to pK^-$ elastic, 2 prong
535	$K^- \to \mu^-\nu_\mu$ decay, $K^-p \to pK^-$ elastic, 2 pr.
538	$K^-p \to \pi^+\pi^-\Lambda^0$, $\Lambda \to p\pi^-$ inelastic, 2 pr. w/vee
541 (8)	$K^-p \to \pi^+\pi^-$ inelastic, 2 pr.
543	$K^-p \to pK^-$, $K^-p \to pK^-$ elastic, elastic, 2 pr.
544	$K^- \to \mu^-\nu_\mu$ decay, $K^-p \to pK^-$ elastic, 2 pr.
545	$K^- \to \mu^-\nu_\mu$ decay, $K^- \to \mu^-\nu_\mu$ decay
550 (10)	$K^-p \to pK^-$; $K^-p \to pK^-$ elastic, elastic, 2 prong
551	$K^-p \to pK^-$; $K^-p \to pK^-$ elastic, elastic, 2 prong
557	$K^- \to \mu^-\nu_\mu$ decay, $K^-p \to pK^-$ elastic, 2 prong
559 (9)	$K^-p \to pK^-$ elastic, 2 prong; $K^- \to \mu^-\nu_\mu$ decay in flight
567	$K^-p \to nK^0$ "disappearance" inelastic
572	$K^-p \to pK^-$, $K^-p \to pK^-$ elastic, elastic 2 prong

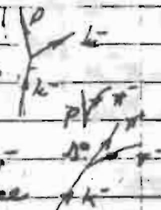

DATA

4-8-96

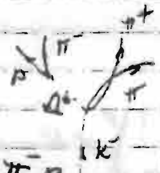

FRAME #	REACTION
575	$K^-p \to \pi^+\pi^-\Lambda^0$ $\hookrightarrow \pi^- p$ inelastic, 2 prong w/vee
576	$K^-p \to pK^-$; $K^-p \to pK^-$ elastic, elastic, 2 prong $K^- \to \mu^-\nu_\mu$ decay
578	$K^- \to \mu^-\nu_\mu$ decay $K^-p \to pK^-$ elastic, 2 prong
579 (10)	$K^-p \to pK^-$ elastic, 2 prong
580	$\boxed{K^- \to \pi^-\pi^-\pi^+}$ 'τ' mode decay
586	$K^- \to \mu^-\nu_\mu$ decay $K^-p \to pK^-$ elastic, 2 prong
591 (8)	$K^-p \to pK^-$ elastic, 2 prong
593	$K^-p \to pK^-$ elastic, 2 prong
594	$K^- \to \mu^-\nu_\mu$ decay
596	$K^-p \to \pi^+\pi^-\Lambda^0$ $\hookrightarrow p\pi^-$ inelastic, 2 prong with vee
601 (9)	$K^- \to \mu^-\nu_\mu$ decay $K^-p \to pK^-$ elastic, 2pr.
603	$K^- \to \mu^-\nu_\mu$ decay $K^-p \to pK^-$ elastic, 2pr. $K^-p \to pK^-$ elastic, 2pr.
606	$K^-p \to pK^-$ elastic, 2pr.
607	$K^-p \to pK^-$ elastic, 2pr.
610 (9)	$K^-p \to pK^-$ elastic, 2pr.
612	$K^-p \to pK^-$ elastic, 2pr. $K^-p \to pK^-$ elastic, 2pr.

FRAME #	REACTION
615	$K^-p \to pK^-$ elastic, 2pr. $K^-p \to pK^-$ elastic, 2pr.
617	$K^-p \to \pi^+\pi^-\Lambda^0$ $\hookrightarrow p\pi^-$ inelastic, 2 prong w/vee
621 (9)	$K^- \to \mu^-\nu_\mu$ decay $K^-p \to pK^-$ elastic, 2pr.
622	$K^- \to \mu^-\nu_\mu$ decay
623	$\boxed{K^- \to \pi^+\pi^-\pi^-}$ decay, τ mode
627	$K^-p \to pK^-$ elastic, 2 prong $K^-p \to pK^-$ elastic, 2 prong
630 (11)	$K^-p \to pK^-$ elastic, 2 prong
631	$K^-p \to pK^-$ elastic, 2 prong $K^-p \to pK^-$ elastic, 2 prong
634	$K^-p \to pK^-$ elastic $K^-p \to pK^-$
637	$K^-p \to pK^-$ elastic, 2pr
642 (8)	$K^-p \to pK^-$, $K^-p \to pK^-$ elastic, elastic, 2pr.
646	$K^- \to \mu^-\nu_\mu$ decay
648	$K^-p \to pK^-$ elastic, 2pr. $K^-p \to pK^-$ elastic, 2pr.
649 (10)	$K^- \to \mu^-\nu_\mu$ decay $K^-p \to pK^-$ elastic, 2 prong
658	$K^- \to \mu^-\nu_\mu$ decay
660 (10)	$K^-p \to pK^-$ elastic, 2pr $K^-p \to pK^-$ elastic

FRAME #	REACTION	FRAME #	REACTION
800	2-Eln	832	2-Eln
801	2,2,2 Eln	835	2,2 Eln
804	2,2, Eln	837	2 Eln
806	2,2,2 Eln	838	2 Eln
807	2,2 Eln	842	2,2 Eln
810	2 Eln	843	5 w/vee - h
811	2 Eln	844	2-Eln
814	2,2,2 Eln	846	5 - h
815	2,2 Eln	848	2,2 Eln
816	2 Eln	849	2,2 Eln
821	2 Eln	850	2-Eln
822	7 - h	854	2-Eln
	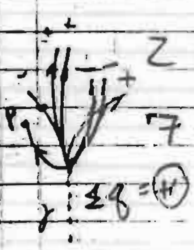	855	2-Eln
		856	7-h
823	2,2 Eln	859	2-Eln
824	2,2 Eln	862	2-Eln
826	7 w/vee - h	864	5-h
	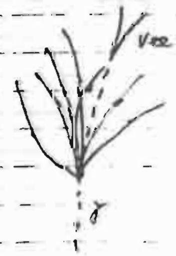	867	2-Eln
		870	2-Eln
		873	2,2 Eln
827	2-Eln	874	2,2 Eln
830	2-Eln	876	3 w/vee - h
831	2 Eln	878	7-h

FRAME #	REACTION	FRAME #	REACTION
884	2,2 Em	945	2,5-h
887	2 Em	947	2-Em
889	2,2 Em	951	3-h
892	2-Em	952	2-Em
894	2,2 Em	954	5-h
896	2-Em	955	7 w/vee -h
898	7-h	956	5 w/vee -h
903	2,2 Em	957	3-h
908	5-h	961	5-h
912	3 w/vee -h	962	2,2 Em
915	7-h	963	5-h
917	7-h	965	-2 Em
919	2-Em	967	-2,2 Em
920	2-Em	969	-2 Em
928	2,2 Em	973	9-h
931	2,2,2,2,2 (Em showers)	974	-5-h
935	3 w/vee -h	980	2-Em
936	7-h		
937	2-Em		
938	2 Em		
939	3-h		
942	2,2 Em		

end.

total number of hadronic photoproduction reactions ≡ 58

total strange particle produced 8